*Canadian Mineralogist*
Vol. 20, pp. 189-202 (1982)

# STILPNOMELANE, IRON-RICH MICA, K-FELDSPAR AND HORNBLENDE IN BANDED IRON-FORMATION ASSEMBLAGES OF THE DALES GORGE MEMBER, HAMERSLEY GROUP, WESTERN AUSTRALIA

TAKASHI MIYANO*
*Department of Geology, Indiana University, Bloomington, Indiana 47405, U.S.A.*

## ABSTRACT

The banded iron-formation of the Dales Gorge Member, Hamersley Group, Western Australia, contains several Al-bearing silicates: stilpnomelane, Fe-rich mica, K-feldspar and hornblende. The mica is flaky to tabular, fine- to medium-grained, and commonly coexists with stilpnomelane, riebeckite, quartz, magnetite, hematite and ankerite. It contains about 1 to 6 wt.% $Al_2O_3$ and 29 to 41 wt.% FeO (total iron as FeO). Angular fragments of hornblende rimmed by riebeckite are dispersed in stilpnomelane–mica bands. K-feldspar with nearly end-member composition occurs in spherulites associated with stilpnomelane and ankerite. Textural relations show that the K–Al silicates and riebeckite are very low-grade metamorphic (or late diagenetic) products, mica and riebeckite having generally formed late and locally replacing stilpnomelane. Textures also suggest that the Al so released may have been reprecipitated as Fe–rich mica close to riebeckite-rich zones. The occurrence of riebeckite and Fe-rich mica may reflect the interaction of alkali-bearing solutions with earlier minerals. The formation of the K–Al minerals may have been controlled by the magnitude of the chemical potential of $K^+$ rather than the temperature of metamorphism. This implies that homogenization of $a_{K+}$ was not attained in the iron formations and that stable associations of the K–Al silicates may have been maintained through local equilibrium.

*Keywords:* very low-grade metamorphism, banded iron-formation, K–Al-bearing silicates, Fe-rich mica (ferriannite), Dales Gorge Member, Western Australia, local equilibrium.

## SOMMAIRE

La formation de fer rubannée du membre Dales Gorge, groupe de Hamersley (Australie occidentale) contient plusieurs silicates alumineux, stilpnomélane, mica ferrifère, feldspath potassique et hornblende. Le mica, de facies feuilleté à tabulaire, de grain fin à moyen, coexiste d'ordinaire avec stilpnomélane, riebeckite, quartz, magnétite et ankérite. Il contient de 1 à 6% (en poids) de $Al_2O_3$ et de 29 à 41% de FeO (fer total exprimé en FeO). Des fragments angulaires de hornblende enrobés de riebeckite sont dispersés dans des lits riches en stilpnomélane et mica. Le feldspath potassique, de composition presque idéale, se présente en sphérolites accompagnés surtout de stilpnomélane et d'ankérite. Les textures montrent que les silicates à K et Al, ainsi que la riebeckite, sont des produits d'un métamorphisme d'intensité très faible (ou de diagenèse tardive) et que mica et riebeckite se sont formés tard et, par endroits, aux dépens de la stilpnomélane. Elles font aussi supposer que l'aluminium ainsi libéré aurait été précipité sous forme de mica ferrifère à proximité des zones à riebeckite. La présence de riebeckite et de mica ferrifère refléterait l'interaction de solutions alcalines avec les minéraux déjà formés. La formation des minéraux à K et Al pourrait bien refléter le potentiel chimique élevé du potassium plutôt que la température du métamorphisme. Ceci impliquerait que l'homogénéisation de l'activité de $K^+$ n'a pas été atteinte dans les formations de fer et que les associations stables des silicates K–Al doivent leur stabilité à un équilibre local.

(Traduit par la Rédaction)

*Mots-clés:* métamorphisme de très faible intensité, formation de fer rubanée, silicates à K et à Al, mica ferrifère (ferriannite), membre Dales Gorge, Australie occidentale, équilibre local.

## INTRODUCTION

The bulk chemistry of Precambrian banded iron-formations is dominated by iron and silica. The content of alumina is generally less than 1 wt. % and that of the alkalis ($Na_2O$ and $K_2O$) may be virtually zero (James & Sims 1973, Gole & Klein 1981). Al-bearing silicates in low-grade metamorphic iron-formations are thus relatively rare. Stilpnomelane is the most common and abundant silicate, but chamosite, Al-greenalite, Fe-chlorite and albite have also been reported from iron formations (*e.g.*, Dimroth & Chauvel 1973, Floran & Papike 1975, 1978, Klein & Fink 1976, Lesher 1978, Gole 1980, Klein & Gole 1981).

Banded iron-formation (BIF) of the Dales Gorge Member, Brockman Iron Formation in

---

*Present address: Institute of Geoscience, The University of Tsukuba, Ibaraki 305, Japan.

the Hamersley Range, Western Australia, which was subjected to very low-grade metamorphism (Miyano 1976b, 1978b), is somewhat different in mineralogy and petrography from other iron formations.

This paper deals with the mineralogy and petrography of silicate-bearing bands of BIF, with special emphasis on the evaluation of textural relations and compositional variations of unusual assemblages such as stilpnomelane–Fe-mica, stilpnomelane–K–feldspar, Fe-rich mica–riebeckite and riebeckite–hornblende. Most samples were taken from drill cores of BIF of the upper Dales Gorge Member at the Colonial Mine in Wittenoom.

## Al-Bearing Silicates

Only small amounts of Al-bearing silicates occur in the BIF of the Dales Gorge Member owing to a low content of alumina, averaging 0.46 wt. % $Al_2O_3$ (Trendall & Blockley 1970). Stilpnomelane, the most abundant Al-bearing silicate (Grubb 1971, Trendall & Blockley 1970, Ayres 1972, Miyano 1976a), may fix almost all aluminum and potassium in the BIF (average 0.12 wt. % $K_2O$: Trendall & Blockley 1970). Other Al-bearing silicates from the BIF, which are usually associated with stilpnomelane, have been reported by several authors. Ayres (1972) described biotite, but without compositional data, from several mesobands (thickness ranging from 2 to 150 mm), where it is intimately associated with stilpnomelane laths. An occurrence similar to this assemblage will be described here. Grubb (1971) reported muscovite and chlorite from the Dales Gorge Member, but his occurrence is confirmed by neither compositional nor X-ray data. Normal biotite, muscovite and chlorite were not noted in this study. If present, they must be very scarce. Figure 1 shows all Al-bearing silicates found in this study.

### *Stilpnomelane*

LaBerge (1966), Trendall & Blockley (1970), Grubb (1971), Ayres (1972) and Miyano (1976a) have all given petrographic descriptions of stilpnomelane from the iron formation of the Dales Gorge Member. Where stilpnomelane is abundant in either a micro- or mesoband, it has a fine grained, acicular habit, and the grains form massive aggregates or networks of interlocking laths (Fig. 2A). The most common mineral assemblage consists principally of stilpnomelane + ankerite + iron oxides + quartz (Fig. 2B), which may be associated with pyrite and siderite, but rarely with Fe-rich mica, riebeckite, pyrrhotite or K-feldspar. Generally the association with Fe-rich mica or riebeckite is restricted to edges of adjoining riebeckite-rich bands. Quartz and hematite are scarce or absent in relatively thick stilpnomelane mesobands. In carbonate-rich (especially ankerite-rich) mesobands, stilpnomelane

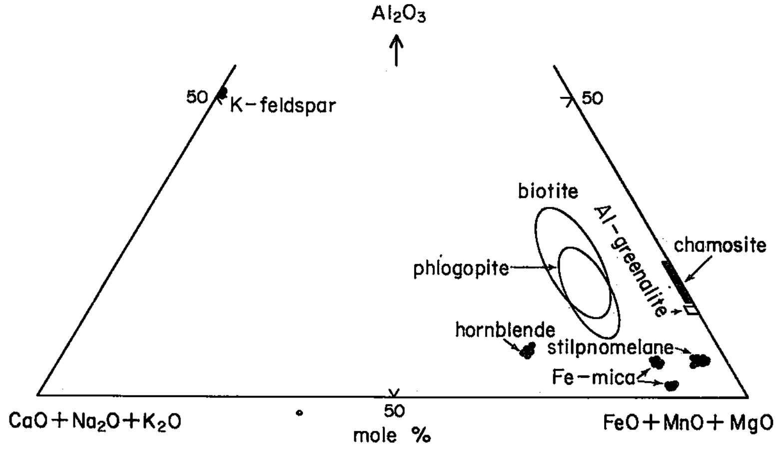

FIG. 1. Summary diagram of Al-bearing silicate compositions. Compositional data for biotite and phlogopite are taken from Deer *et al.* (1962) and those for chamosite and Al-greenalite, from Klein & Fink (1976) and Floran & Papike (1975). All other data are from the present study. FeO in Figures 1, 3, 5, 7, and 9 means total Fe recalculated as FeO. Fe-mica: Fe-rich mica.

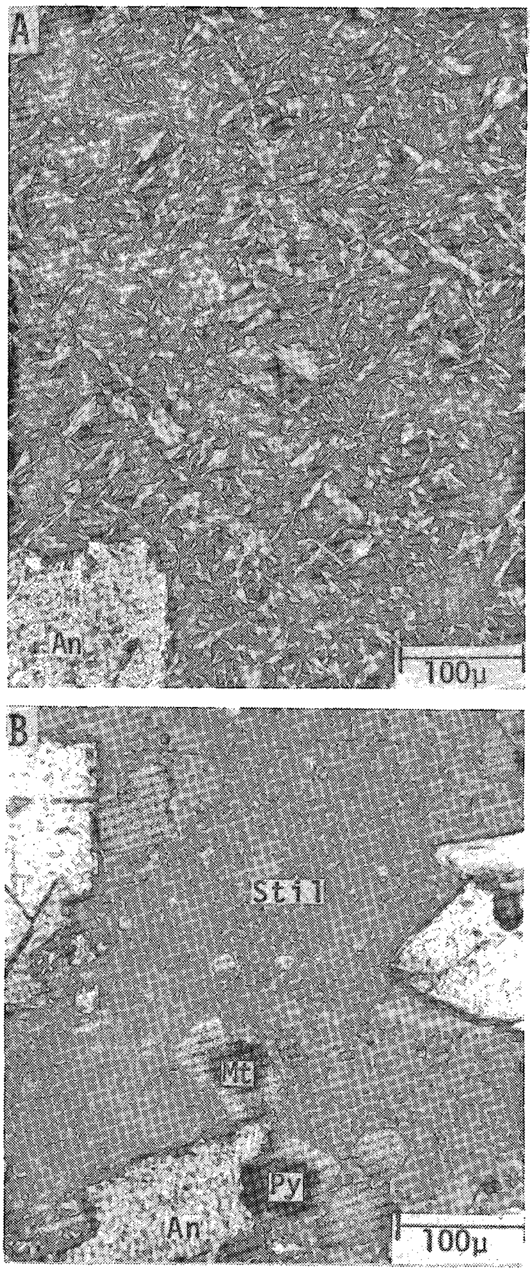

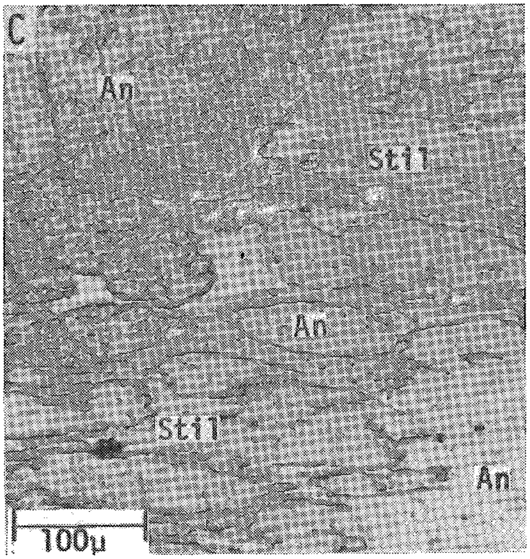

FIG. 2. Stilpnomelane occurrences. A. Networks of interlocking laths of ferrostilpnomelane. Doubly polarized light. An: ankerite. B. Massive aggregates of ferristilpnomelane, which lack hematite and quartz. Polarized light. Stilpnomelane (Stil) coexists with ankerite (An), magnetite (Mt) and pyrite (Py). C. Irregular aggregates of ferristilpnomelane (Stil) interstitial to ankerite rhombs (An). The opaque mineral is magnetite. Polarized light. Aggregates lie nearly parallel to the sedimentary banding.

commonly forms irregular aggregates interstitial to ankerite rhombs that are nearly parallel to the sedimentary banding (Fig. 2C). The X-ray powder-diffraction pattern of this stilpnomelane shows an extra peak at $d = 9.41$ Å that may be the equivalent to $d_{002}$ of minnesotaite. Massive aggregates or continuous layers of stilpnomelane are rare in iron-oxide-rich mesobands. Instead, an acicular variety occurs next to the grain boundaries of iron oxides. Discontinuous layers of lenticular aggregates of stilpnomelane less than 0.1 mm thick are common in chert mesobands; such layers are commonly broken by intervening recrystallized quartz.

The chemical composition of the stilpnomelane can be described entirely by $K_2O$, FeO, MgO, $Fe_2O_3$, $Al_2O_3$ and $SiO_2$. Other components are minor and total less than 1% (Table 1). The stilpnomelane formula is recalculated on the basis of 22 oxygen atoms in order to compare with that of Fe-rich mica. Compositional diagrams for stilpnomelane and associated minerals are given in Figures 1, 3, 7 and 9. The largest range of chemical variation is caused by variable $Fe^{2+}$ and $Fe^{3+}$ contents (Deer *et al.* 1962). The $Fe^{2+}$-rich variety, ferrostilpnomelane, has pale green pleochroic colors; the $Fe^{3+}$-rich one, ferristilpnomelane, has brown to dark brown pleochroic colors. The $d_{001}$ of ferrostilpnomelane ranges from 11.98 to 11.99 Å, and that of ferristilpnomelane, from 12.14 to 12.28 Å, as determined by X-ray powder diffraction. $Fe^{2+}$ and $Fe^{3+}$ cannot be distinguished by electron-microprobe analysis, but complete analyses by Trendall & Blockley (1970) give

TABLE 1. REPRESENTATIVE MICROPROBE ANALYSES OF AL-BEARING SILICATES IN BANDED IRON-FORMATION OF THE DALES GORGE MEMBER

| | 1 | 2 | 3 | 4 | 5 | 6 | 7 | 8 | 9 | 10 |
|---|---|---|---|---|---|---|---|---|---|---|
| wt. % | FH7 | J294 | B402 | Z262 | DE2 | Z128 | M376 | Z80 | Z122 | FH5 |
| $SiO_2$ | 45.71 | 44.82 | 48.40 | 47.61 | 38.39 | 38.69 | 35.09 | 47.85 | 48.62 | 65.43 |
| $Al_2O_3$ | 5.35 | 4.62 | 4.44 | 4.19 | 4.99 | 5.52 | 1.83 | 7.72 | 6.71 | 18.14 |
| $TiO_2$ | 0.06 | 0.01 | 0.01 | 0.02 | 0.00 | 0.08 | 0.00 | 1.41 | 1.51 | 0.00 |
| $Cr_2O_3$ | n.d. | n.d. | 0.00 | 0.00 | n.d. | 0.00 | n.d. | 0.01 | 0.02 | n.d. |
| FeO* | 33.05 | 31.86 | 25.65 | 26.45 | 30.86 | 29.47 | 40.99 | 12.06 | 13.27 | 0.18 |
| MnO | 0.12 | 0.00 | 0.03 | 0.10 | 0.09 | 0.04 | 0.01 | 0.36 | 0.49 | 0.02 |
| NiO | n.d. | n.d. | 0.06 | 0.00 | n.d. | 0.00 | n.d. | 0.00 | 0.00 | n.d. |
| MgO | 3.82 | 4.94 | 9.55 | 9.43 | 12.25 | 11.84 | 7.73 | 15.37 | 14.43 | 0.00 |
| CaO | 0.04 | 0.02 | 0.04 | 0.01 | 0.02 | 0.00 | 0.00 | 10.78 | 10.88 | 0.02 |
| $Na_2O$ | 0.32 | 0.01 | 0.23 | 0.04 | 0.03 | 0.03 | 0.00 | 1.69 | 1.80 | 0.07 |
| $K_2O$ | 1.83 | 2.96 | 2.89 | 1.75 | 8.76 | 8.33 | 7.85 | 0.36 | 0.56 | 16.26 |
| Total | 90.30 | 89.24 | 91.30 | 89.60 | 95.39 | 94.00 | 93.50 | 97.61 | 98.29 | 100.12 |
| Fe/(Fe+Mg) | 0.829 | 0.778 | 0.605 | 0.611 | 0.586 | 0.583 | 0.751 | 0.306 | 0.340 | ------ |
| | Number of ions on the basis of 22 oxygens | | | | | | | 23 oxygens | | 8 oxygens |
| Si | 7.398 | 7.372 | 7.470 | 7.477 | 6.238 | 6.308 | 6.214 | 6.956 | 7.070 | 3.016 |
| Al | 0.602 | 0.628 | 0.530 | 0.523 | 0.956 | 1.061 | 0.382 | 1.044 | 0.930 | 0 |
| Σ | 8.000 | 8.000 | 8.000 | 8.000 | 7.194 | 7.369 | 6.596 | 8.000 | 8.000 | 3.016 |
| Al | 0.419 | 0.268 | 0.278 | 0.253 | 0.000 | 0.000 | 0.000 | 0.280 | 0.220 | 0.986 |
| Ti | 0.007 | 0.001 | 0.001 | 0.002 | 0.000 | 0.010 | 0.000 | 0.154 | 0.165 | 0.000 |
| Cr | ----- | ----- | 0.000 | 0.000 | ----- | 0.000 | ----- | 0.001 | 0.002 | ----- |
| $Fe^{2+}$ | 4.474 | 4.383 | 3.311 | 3.474 | 4.194 | 4.019 | 6.071 | 1.466 | 1.614 | 0.007 |
| Mn | 0.016 | 0.000 | 0.004 | 0.013 | 0.012 | 0.006 | 0.002 | 0.044 | 0.060 | 0.001 |
| Ni | ----- | ----- | 0.007 | 0.000 | ----- | 0.000 | ----- | 0.000 | 0.000 | ----- |
| Mg | 0.921 | 1.211 | 2.197 | 2.207 | 2.967 | 2.877 | 2.040 | 3.330 | 3.127 | 0.000 |
| Σ | | | | | 7.173 | 6.912 | 8.113 | 5.275 | 5.188 | 0.994 |
| Ca | 0.007 | 0.004 | 0.007 | 0.002 | 0.003 | 0.000 | 0.000 | 1.679 | 1.695 | 0.001 |
| Na | 0.100 | 0.003 | 0.069 | 0.012 | 0.009 | 0.009 | 0.000 | 0.476 | 0.507 | 0.006 |
| K | 0.378 | 0.621 | 0.569 | 0.351 | 1.816 | 1.733 | 1.774 | 0.067 | 0.104 | 0.956 |
| Σ | 6.322 | 6.491 | 6.443 | 6.314 | 1.828 | 1.742 | 1.774 | 2.222 | 2.306 | 0.963 |

1) Acicular to fibrous ferrostilpnomelane associated with pyrite and pyrrhotite in spherical aggregates of K-feldspar (see Fig. 8). 2) Ferrostilpnomelane associated with pyrite and magnetite, forming networks of interlocking laths (see Fig. 2A ). 3) Ferrostilpnomelane associated with hematite and quartz, locally magnetite, ankerite, and siderite, forming a thin lenticular and discontinuous band. 4) Brown ferristilpnomelane associated with Fe-rich mica, dispersed magnetite and amphiboles (see Fig. 6 ). 5) Flaky grain of Fe-rich mica associated with hematite, magnetite, ankerite, quartz, and riebeckite in a chert mesoband. 6) Flaky grain of Fe-rich mica forming thin bands which alternate with hematite+ magnetite-bearing microbands. 7) Massive aggregate of Fe-rich mica associated with hematite, quartz, and ankerite, locally riebeckite prisms and magnetite, forming a lenticular and discontinuous band (see Fig. 4B). 8) Hornblende surrounded by riebeckite (see Fig. 6). 9) Same as 8. 10) Spherical aggregate of K-feldspar (see Fig. 8). *All Fe reported as FeO.

$Fe_2O_3$ contents of ferro- and ferristilpnomelane as 2.90 and 18.49 wt. %, respectively. However, ferrostilpnomelane is easily altered to ferristilpnomelane by oxidation (Miyano 1976a). Ayres (1972) noted from his microprobe analyses that ferristilpnomelane has a higher Fe content than ferrostilpnomelane. The chemical analyses obtained in this study do not confirm this finding. The pale green variety has a similar total FeO content to Ayres's ferristilpnomelane (36.63 wt. % FeO), and the brown variety has a similar total FeO content to Ayres's ferrostilpnomelane (21.94 wt. % FeO). Owing to the ease of oxidation of $Fe^{2+}$ to $Fe^{3+}$ in the relatively open structure of stilpnomelane (Eggleton 1972), it is very likely that the brown to dark brown stilpnomelane is of secondary origin and that all primary stilpnomelane originated as ferrostilpnomelane. The possibility of a secondary origin for the high $Fe^{3+}$ contents in stilpnomelane has been proposed by many workers (*e.g.*, Klein 1974, Floran & Papike 1975, Gole 1980). It appears that the wide range of $d_{001}$ of ferristilpnomelane is a reflection of different degrees of oxidation. It is evident that brown ferristilpnomelane has a lower iron content (about 23 to 27 wt. % total FeO) than the dark brown variety, which has more than 30 wt. % total FeO (Table 1). It may be that very iron-rich stilpnomelane is more easily oxidized to ferristilpnomelane than a relatively iron-poor variety because of the inherently higher content of ferrous iron. The $K_2O$ content of stilpnomelane in iron-formation

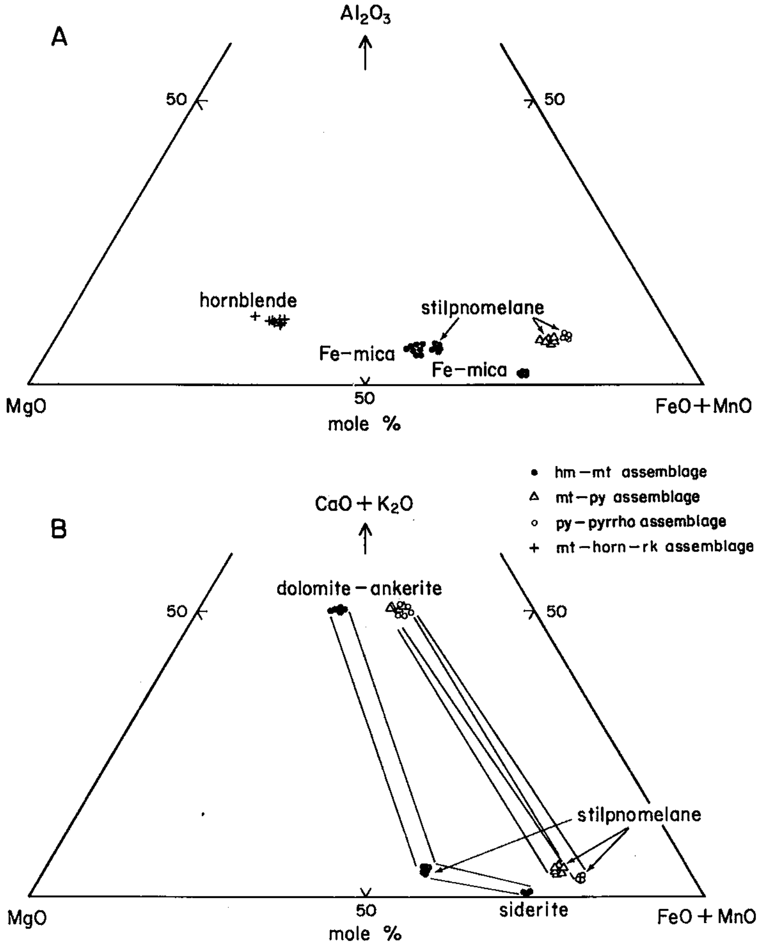

FIG. 3 A. Compositional variation of hornblende, Fe-rich mica, and stilpnomelane in banded iron-formation of the Dales Gorge Member. Fe-mica: Fe-rich mica. One group of Fe-rich mica (Table 1, columns 5, 6) has a similar $Al_2O_3$ content to that of stilpnomelane (Table 1, columns 1 to 4) but contains more alumina and less iron than another group (Table 1, column 7). The compositional variation shown by stilpnomelane reflects the differences in the mineral assemblages (see text, also Fig. 3B). B. Variations in stilpnomelane compositions as a function of differing assemblages. Generally, assemblages with hematite and magnetite have a higher Mg/(Mg+Fe) ratio than those with magnetite and pyrite or with pyrite and pyrrhotite.

rocks generally ranges from 1.0 to 2.0 wt. % (*e.g.*, Klein 1974, Klein & Fink 1976, Floran & Papike 1975, 1978). However, in the Dales Gorge Member, the $K_2O$ content often exceeds 2 wt. % (Table 1, columns 2,3), especially in stilpnomelane that occurs near or within riebeckite-rich zones. Preliminary analytical data show that the $K_2O$ content of such stilpnomelane ranges from 1 to 6 wt. %.

### *Fe-rich mica*

Iron-rich and Al-poor mica, as first described from this Precambrian iron-formation, refers to mica with an $Al_2O_3$ content that is lower by 5 to 10 wt. % than that of average biotite or phlogopite (Table 1, Fig. 1). The $d_{001}$ value in such mica, as obtained by X-ray powder diffraction, ranges from 10.14 to 10.16

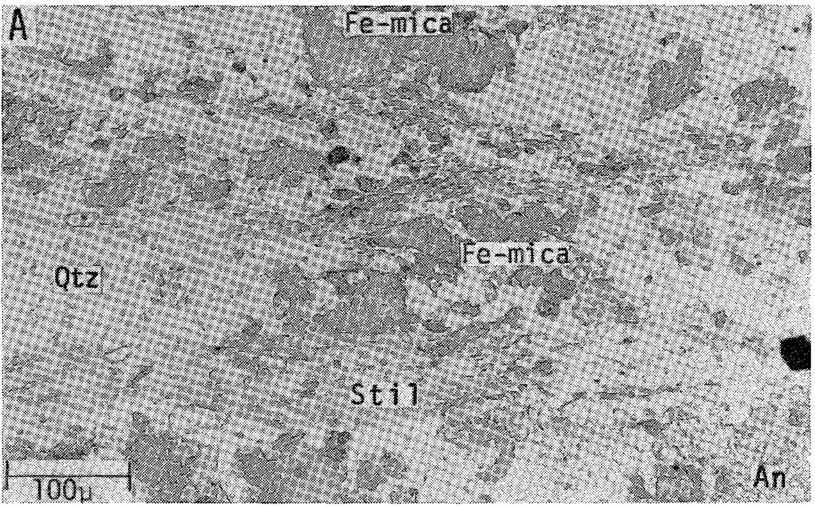

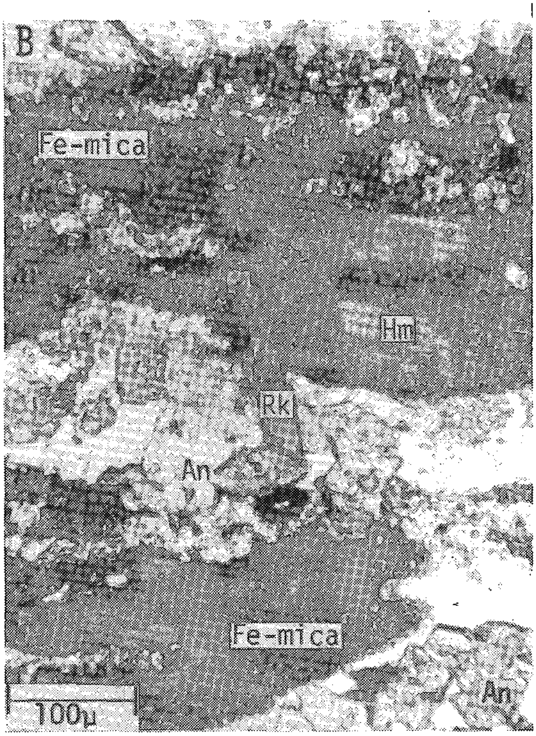

FIG. 4. Fe-rich mica occurrences. A. Dispersed grains of Fe-rich mica (Fe-mica) in a chert mesoband. Stilpnomelane (Stil) grains are subparallel to the banding. Polarized light. The scale in A is the same as in B. B. Massive aggregates of Fe-rich mica form lenticular bands, one of which is traversed by a prismatic riebeckite grain (Rk). Elongate grains of hematite (black, Hm) are enclosed within the bands. Polarized light. Mica has a lower $Al_2O_3$ content than that shown in A (Table 1, column 7).

Å, and is slightly larger than that of biotite or phlogopite.

The textural appearance of this Fe-rich mica is similar to that of stilpnomelane, but it is generally more coarsely crystallized than stilpnomelane. Flaky and tabular grains range from 10 to 40 μm in diameter and are dispersed in chert-rich mesobands (Fig. 4A), associated with ankerite, hematite, magnetite, stilpnomelane, quartz and riebeckite. In most occurrences, the mica is closely associated with riebeckite-rich bands; it is usually concentrated in those that parallel the overall banding. Thin (0.2 mm across) Fe-rich-mica layers alternate with iron-oxide microbands or form discontinuous lenses with elongated hematite grains and are crossed by prismatic riebeckite grains (Fig. 4B). It appears that such bands may originally have been stilpnomelane bands, because stilpnomelane is replaced by Fe-rich mica in many occurrences where they coexist. The Fe-rich mica also occurs as thin veinlets developed from stilpnomelane bands. The occurrence is similar to a veinlet of biotite-like material reported by Klein & Gole (1981) from the Marra Mamba Iron Formation, Hamersley Group, 300 m lower than the Dales Gorge Member. However, that material is more Al-rich and Fe-poor than the mica in this study.

Fe-rich mica and riebeckite generally appear to be later than any of the other minerals, but the mica itself is in places cut by riebeckite prisms that also cut across acicular or fibrous riebeckite-rich bands. It may be that fibrous riebeckite is essentially contemporaneous with the mica.

The chemical composition of the Fe-rich

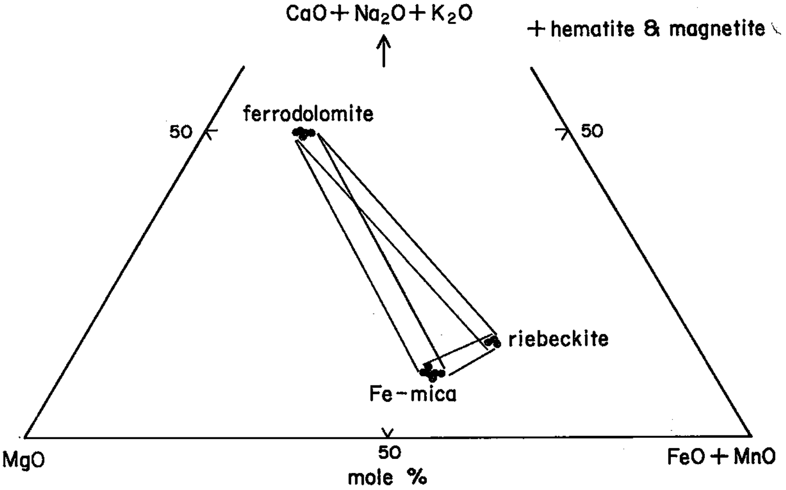

FIG. 5. Compositional variation of the assemblage ferrodolomite + riebeckite + Fe-rich mica (Fe-mica). The assemblage also contains hematite magnetite and quartz.

mica is similar to that of stilpnomelane, but with a higher $K_2O$ and a lower $SiO_2$ content than stilpnomelane. Results of electron-microprobe analyses are given in Table 1, and compositional diagrams are shown in Figures 1, 3A, 5 and 7. The mica occurs in two colored varieties, one with light reddish brown (*X*) to pale yellow green (*Y*,*Z*) pleochroism and the other with brownish red (*X*) to pale greenish brown (*Y*,*Z*) pleochroic colors. Table 1 shows that the latter variety (column 7) has a higher FeO content by about 10 wt. % and a lower $Al_2O_3$ content by about 3 wt. % than the former (columns 5, 6). It is likely that the reddish brown (*X*) to deep green (*Y*,*Z*) variety is a product of secondary oxidation of the former type because both varieties give almost identical electron-probe analyses. The number of ions in the mica, recalculated on the basis of 22 oxygen atoms, shows a cation deficiency in the tetrahedral sites and a cation excess in the octahedral sites. Assuming that the deficiency is filled with $Fe^{3+}$ for 8 cations, the number of octahedral cations becomes 6.05, 6.03, and 6.16 for specimens 5, 6 and 7 in Table 1, respectively. Such values, larger than 6, can be caused by a lower $K_2O$ content than in ideal mica. It is possible that the tetrahedral Al-position is in part substituted for by ferric iron. Synthetic Al-free mica ("ferri-annite") $K_2Fe^{2+}{}_6Fe^{3+}{}_2Si_6O_{20}(OH)_4$ ($d_{001}$ 10.16 ~ 10.18 Å) has been described by Wones (1963) and Donnay *et al.* (1964). This may be considered an end member for this Fe-rich mica.

Results of chemical analyses of stilpnomelane, ankerite (ferrodolomite) and riebeckite coexisting with the mica are given in Tables 1, 2 and 3. The compositional variations of ferrodolomite + Fe-rich mica + riebeckite and of stilpnomelane + Fe-rich mica + riebeckite + hornblende are shown in Figures 5 and 7,

TABLE 2. REPRESENTATIVE MICROPROBE ANALYSES OF CARBONATES IN BANDED IRON-FORMATION OF THE DALES GORGE MEMBER

| | 1 | 2 | 3 | 4 | 5 |
|---|---|---|---|---|---|
| wt. % | DE29 | B460 | J319 | FH34 | B466 |
| $SiO_2$ | 0.18 | 0.16 | 0.18 | 0.31 | 0.14 |
| $Al_2O_3$ | 0.00 | 0.00 | 0.01 | 0.00 | 0.00 |
| $TiO_2$ | 0.00 | 0.00 | 0.02 | 0.04 | 0.02 |
| $Cr_2O_3$ | n.d. | 0.00 | n.d. | n.d. | 0.03 |
| FeO* | 10.37 | 14.72 | 20.29 | 19.51 | 49.23 |
| MnO | 0.58 | 0.00 | 1.31 | 0.69 | 0.28 |
| NiO | n.d. | 0.00 | n.d. | n.d. | 0.06 |
| MgO | 16.06 | 12.15 | 7.56 | 7.59 | 9.66 |
| CaO | 28.49 | 28.33 | 27.50 | 27.81 | 0.13 |
| $Na_2O$ | 0.02 | 0.00 | 0.00 | 0.00 | 0.07 |
| $K_2O$ | 0.00 | 0.00 | 0.00 | 0.09 | 0.00 |
| Total | 55.70 | 55.36 | 56.87 | 56.04 | 59.62 |
| Fe/(Fe+Mg) | 0.266 | 0.405 | 0.601 | 0.591 | 0.740 |
| | Number of ions on the basis of 2 oxygens | | | | |
| $Fe^{2+}$ | 0.273 | 0.405 | 0.577 | 0.563 | 1.472 |
| Mn | 0.015 | 0.000 | 0.038 | 0.020 | 0.008 |
| Mg | 0.752 | 0.596 | 0.383 | 0.390 | 0.515 |
| Ca | 0.960 | 0.999 | 1.002 | 1.027 | 0.005 |
| ΣCations | 2.000 | 2.000 | 2.000 | 2.000 | 2.000 |

1) Medium-grained, euhedral ferrodolomite, associated with quartz, hematite, magnetite, riebeckite, and Fe-rich mica in a chert mesoband. 2) Medium- to coarse-grained, euhedral ferrodolomite, associated with quartz, hematite, siderite, ferrostilpnomelane, and locally magnetite in a quartz-iron oxide mesoband. 3) Medium-grained, euhedral ankerite, associated with dispersed pyrite and magnetite in a matrix of interlocking laths of ferrostilpnomelane (see Fig. 2 ). 4) Medium-grained, subhedral ankerite, associated with pyrite, pyrrhotite, and ferrostilpnomelane in a spherical aggregate of K-feldspar (see Fig. 8). 5) Fine- to medium-grained, subhedral siderite, associated with hematite, ferrostilpnomelane, and locally magnetite in a quartz-iron oxide mesoband. *All Fe as FeO.

TABLE 3. REPRESENTATIVE MICROPROBE ANALYSES OF RIEBECKITE IN BANDED IRON-FORMATION OF THE DALES GORGE MEMBER

|  | 1 |  | 2 |  | 3 |  |
|---|---|---|---|---|---|---|
| wt. % | Z78 |  | Z121 |  | DE2 |  |
| $SiO_2$ | 51.89 |  | 52.25 |  | 54.46 |  |
| $Al_2O_3$ | 0.45 |  | 0.33 |  | 0.05 |  |
| $TiO_2$ | 0.65 |  | 1.00 |  | 0.01 |  |
| $Cr_2O_3$ | 0.00 |  | 0.00 |  | n.d. |  |
| FeO* | 33.74 |  | 33.39 |  | 27.12 |  |
| MnO | 0.00 |  | 0.03 |  | 0.04 |  |
| NiO | 0.01 |  | 0.01 |  | n.d. |  |
| MgO | 2.89 |  | 2.73 |  | 7.76 |  |
| CaO | 0.15 |  | 0.19 |  | 0.14 |  |
| $Na_2O$ | 6.72 |  | 5.87 |  | 6.41 |  |
| $K_2O$ | 0.22 |  | 0.18 |  | 0.08 |  |
| Total | 96.72 |  | 95.98 |  | 96.07 |  |
| Fe/(Fe+Mg) | 0.868 |  | 0.873 |  | 0.662 |  |
| Number of ions on the basis of 23 oxygens |  |  |  |  |  |  |
| Si | 8.236 | 8.24 | 8.309 | 8.31 | 8.366 | 8.37 |
| Al | 0.000 |  | 0.000 |  | 0.000 |  |
| Al | 0.084 | 5.33 | 0.062 | 5.28 | 0.009 | 5.28 |
| Ti | 0.078 |  | 0.120 |  | 0.001 |  |
| Cr | 0.000 |  | 0.000 |  | ----- |  |
| $Fe^{2+}$ | 4.479 |  | 4.441 |  | 3.484 |  |
| Mn | 0.000 |  | 0.004 |  | 0.005 |  |
| Ni | 0.001 |  | 0.001 |  | ----- |  |
| Mg | 0.684 |  | 0.647 |  | 1.777 |  |
| Ca | 0.026 | 2.14 | 0.032 | 1.88 | 0.023 | 1.95 |
| Na | 2.068 |  | 1.810 |  | 1.909 |  |
| K | 0.045 |  | 0.037 |  | 0.016 |  |

1) Riebeckite surrounding an angular fragment of hornblende (see Fig. 6). 2) Same as 1. 3) Fibrous riebeckite associated with Fe-rich mica, ferrodolomite, hematite, and magnetite in a chert mesoband. *All Fe as FeO.

respectively. Figure 7 shows that the ratios of Fe/(Fe+Mg) of the Fe-rich mica and the associated stilpnomelane are almost identical because the Mn contents of both minerals are virtually zero.

### *Hornblende*

Angular fragments of hornblende occur in stilpnomelane-rich mesobands of the iron formation along contacts with hematite–magnetite–Fe-rich-mica bands. Hornblende grains rimmed by riebeckite are dispersed in a matrix of acicular stilpnomelane and Fe-rich mica, associated with euhedral magnetite grains and interstitial patches of quartz (Fig. 6). The hornblende plays the part of a seed for riebeckite overgrowths. The pleochroism of the hornblende is difficult to determine because of blue to yellowish green pleochroic colors of the rimming riebeckite. A similar textural occurrence of these two minerals is described by Milton & Eugster (1959) in the Green River Formation. There, light blue, secondary riebeckite has formed as rims around detrital, brown hornblende grains. Ayres (1972) also noted that some angular fragments of amphibole from the BIF of the Dales Gorge Member appear to be partly replaced by blue riebeckite.

Results of electron-probe analyses of the central hornblende and the rimming riebeckite are given in Tables 1 (columns 8,9) and 3, and they are shown graphically in Figures 3A and 7. Figure 7 gives the compositional range of minerals in the assemblage hornblende + riebeckite + stilpnomelane + Fe-rich mica.

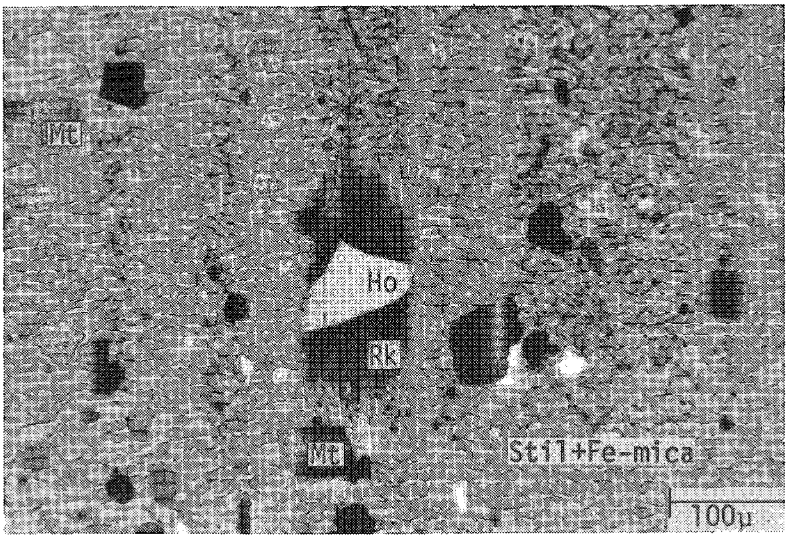

FIG. 6. Hornblende occurrences in a stilpnomelane-rich band. Angular grain of hornblende (Ho) surrounded by riebeckite (Rk). Euhedral grains of magnetite (black, Mt) are dispersed through the stilpnomelane and Fe-rich mica matrix. Polarized light.

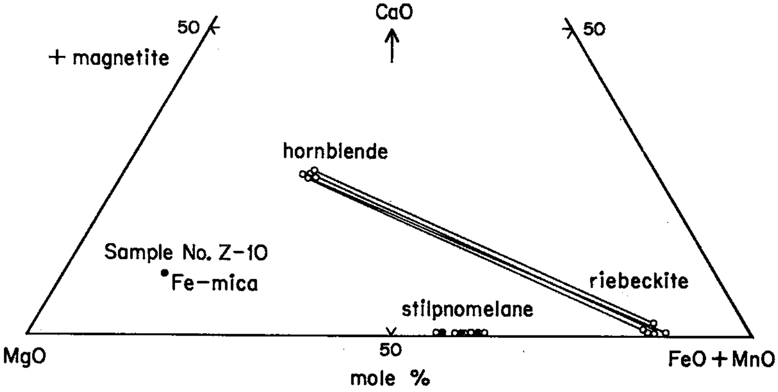

FIG. 7. Compositional variations of hornblende cores and riebeckite rims. The compositions of associated stilpnomelane and Fe-rich mica (solid circle) are also shown.

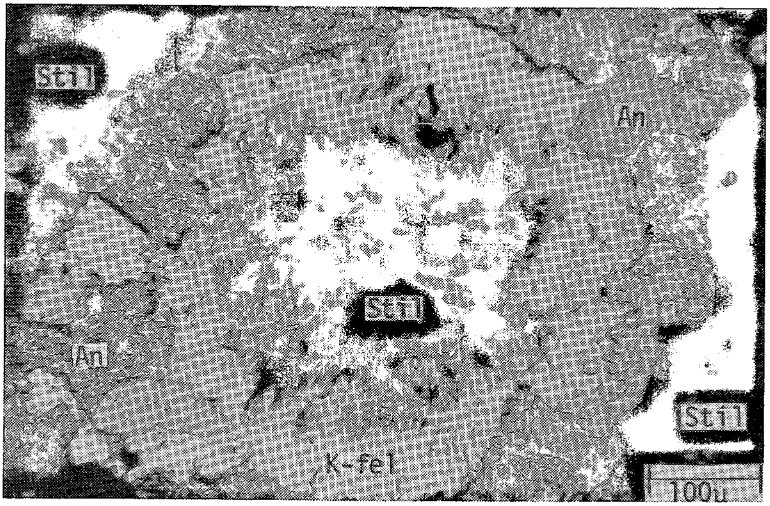

FIG. 8. K-feldspar occurrences in a stilpnomelane-rich band. Spherical aggregates of K-feldspar (K-fel) around a fibrous to acicular stilpnomelane (Stil) core and surrounded by ankerite rhombs (An). Polarized light.

*K-feldspar*

K-feldspar occurs in spherulites with a diameter of up to 3 mm; these are dispersed in a 3-cm-thick stilpnomelane-rich band. The spherulites consist of three distinct parts: a core, middle, and outer rim. K-feldspar is present in the middle as a concentric aggregate of radiating sprays and mosaic forms (Fig. 8). The core consists mainly of aggregates of stilpnomelane with fibrous or acicular spray texture. The rims of the spherules are made up of ankerite rhombs. Small amounts of pyrite, pyrrhotite and, rarely, magnetite are dispersed throughout the spherulites.

The main chemical components, as shown by microprobe analyses, are $K_2O$, $Al_2O_3$ and $SiO_2$. Other components total less than 1% (Table 1, column 10). Results of representative electron-probe analyses of ankerite and stilpnomelane coexisting with the feldspar are given in Tables 1 and 2. Compositional relations of the assemblage K-feldspar + ankerite + stilpnomelane are shown in Figure 9.

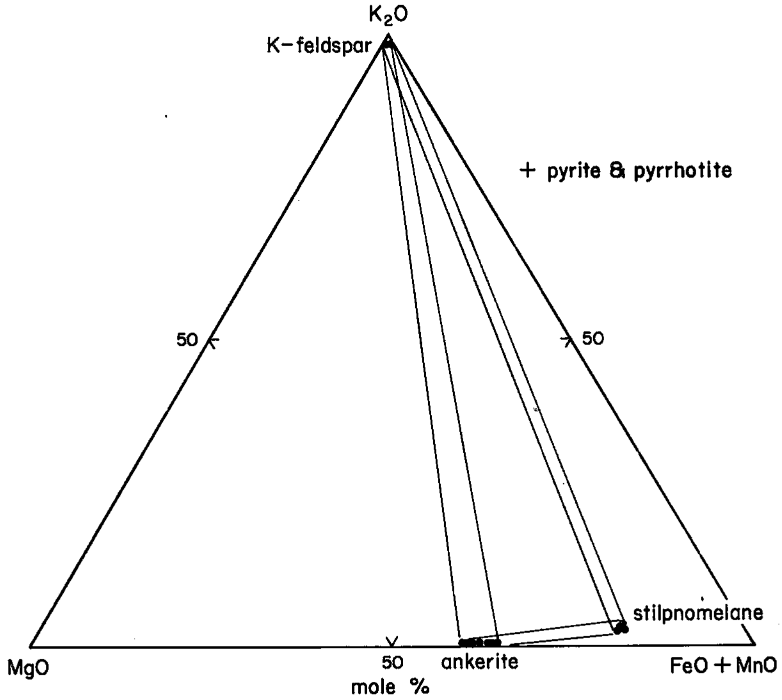

FIG. 9. Compositional variation of the assemblage K-feldspar + ankerite + ferrostilpnomelane. The assemblage also contains pyrite and pyrrhotite.

## DISCUSSION

### *Fe/(Fe+Mg) ratio*

The possible relationship between the Fe/(Fe+Mg) ratio of a specific mineral and the variety of assemblages in which it occurs was evaluated for all silicates and carbonates reported here. The significance of the relationship between $f(O_2)$ and Fe/(Fe+Mg) in iron silicates has been noted by many authors (*e.g.*, Mueller 1960, Burt 1972, Miyano 1976b, Frost 1979). There are remarkable differences in such relationships for stilpnomelane, riebeckite and ankerite. Stilpnomelane associated with both hematite and magnetite (but hematite dominant) contains 23 to 27 wt. % total FeO; note that the total iron expressed as FeO would reflect mainly ferrous iron as already discussed. Stilpnomelane coexisting with both magnetite and pyrite or both pyrite and pyrrhotite has 31 to 36 wt. % total FeO. This implies that the Fe/(Fe+Mg) ratio of stilpnomelane tends to increase with decreasing oxygen (or sulfur) fugacity at constant $P(CO_2)$ and $P(H_2O)$, and that the magnitude of $f(O_2)$ or $f(S_2)$ is locally variable through the entire iron-formation member. In further discussion, the Fe/(Fe+Mg) ratio can be regarded as a function of $f(O_2)$ only, because $f(S_2)$ is directly dependent on $f(O_2)$ in the mineral assemblages of the Dales Gorge Member (Miyano 1976b). A similar conclusion has been reached for minnesotaite in the Dales Gorge Member by Miyano (1978a). However, the Fe/(Fe+Mg) ratio of minnesotaite seems to be more senstive to the magnitude of $f(O_2)$ than that of stilpnomelane. If reduction has taken place during metamorphism (Miyano 1976b), stilpnomelane with a high Fe/(Fe+Mg) ratio may have recrystallized from one with a lower ratio by enrichment in ferrous iron.

The Fe/(Fe+Mg) ratio of riebeckite in a hematite–ferrodolomite association (Table 3, column 3; also see Fig. 5) is lower than the ratio in an association including neither hematite nor carbonates (Table 3, columns 1, 2; also see Fig. 7). The presence of hematite, however, does not appear to affect the Fe/(Fe+Mg) ratio much, judging from these preliminary compositional data.

Members of the dolomite–ankerite series

$CaMg(CO_3)_2$–$CaFe(CO_3)_2$ have variable Fe/(Fe+Mg) ratios depending on the variety of mineral assemblages in which they occur, as shown in Figure 3B. In some occurrences of the same assemblage, however, the Fe/(Fe+Mg) ratios of the carbonates are apparently different, which can be seen by comparing Figures 3B and 5. Generally, the Fe/(Fe+Mg) ratios of carbonates have a wider range than those of coexisting silicates (Miyano 1976a, 1978a, Klein & Gole 1981).

### *Possible reactions and stability relations*

Because of a lack of experimental and thermochemical data, the stability relations of Al-bearing silicates reported here cannot be evaluated quantitatively. The mineral assemblages can be used, however, to provide some qualitative stability-relations for these minerals by considering an additional Al-bearing silicate assemblage reported by other authors. LaBerge (1966, p. 159) noted a possible montmorillonite (nontronite?)–stilpnomelane assemblage in the rocks of the Dales Gorge Member. He concluded that stilpnomelane might have formed from nontronite. Trendall & Blockley (1970, p. 115) also reported montmorillonoid from a shale macroband, suggesting that the montmorillonite was earlier misidentified as chlorite under the microscope.

Qualitative phase-relations of Al-bearing silicates may be evaluated by proposing possible chemical reactions among them. Simplified chemical formulae for such silicates are as follows: nontronite $Fe^{3+}_{3.97}Al_{0.92}Si_{7.34}O_{20}(OH)_4 \cdot mH_2O$, stilpnomelane $K_{0.55}Fe^{2+}_{5.45}Al_{0.93}Si_{7.44}O_{20}(OH)_4 \cdot mH_2O$, Fe-rich mica $K_{1.80}Fe^{2+}_{6.06}Fe^{3+}_{1.16}Al_{0.76}Si_{6.08}O_{20}(OH)_4$ and K-feldspar $KAlSi_3O_8$. The formulae of stilpnomelane and Fe-mica represent their average compositions, with ratios of Si/Al nearly equal to 8. Recalculated on the basis of 15.6 cations, the former is almost equivalent to $K_{0.6}Fe_6(AlSi_8)O_{20}(O,OH)_{27} \cdot \sim 2H_2O$ of Eggleton & Chappell (1978). Because the chemical composition of nontronite in iron formations has not been determined, the formula assumes Si/Al=8, as based upon the generalized formula of Sudo (1974). Nontronite usually contains a considerable amount of ferric iron (Deer *et al.* 1962), and interlayer cations may be regarded as virtually absent in the simplified formula. Using mineral assemblages, textural relations, and the above simplified formulae for the Al-bearing silicate, possible generalized reactions are as follows: 1) 1.01 nontronite + 1.43(Fe) + $0.55K^+$ = stilpnomelane + $m(1)H_2O$ + $0.55H^+$ + $n(1)O_2$, 2) stilpnomelane + 3.36(Fe) + $1.65K^+$ = 1.22 Fe-rich mica + $m(2)H_2O$ + $1.65H^+$ + $n(2)O_2$ and 3) stilpnomelane + $0.38K^+$ = 0.93 $KAlSi_3O_8$ + $4.65SiO_2$ + 5.45(Fe) + $m(3)H_2O$ + $0.38H^+$ + $n(3)O_2$, where (Fe) implies iron oxides (or sulfides). The stoichiometric coefficients of water ($m$) and oxygen (or sulfur) ($n$) are dependent upon the unknown number of $H_2O$ in nontronite and stilpnomelane, and upon the variety of (Fe), respectively.

Each reaction described above proceeds to the right with an increasing activity ratio $a_{K^+}/a_{H^+}$ at constant $f(O_2)$ [or $f(S_2)$], $f(H_2O)$ and T. Two reaction sequences for the silicates discussed may be suggested with increasing $a_{K^+}/a_{H^+}$ at constant $f(O_2)$ [or $f(S_2)$], $f(H_2O)$ and T: nontronite→stilpnomelane→K-feldspar and nontronite→stilpnomelane→Fe-rich mica (Fig. 10). Such a sequence has been determined in the system $K_2O$–$Al_2O_3$–$SiO_2$–$H_2O$ by Hemley (1959) and Helgeson *et al.* (1969). They showed the sequences of kaolinite→K-mica→K-feldspar and kaolinite→K-montmorillonite→muscovite→microcline with increasing $a_{K^+}/a_{H^+}$, keeping other parameters fixed.

The $a_{K^+}/a_{H^+}$ ratio may be one of the most effective parameters for determining such reaction sequences of Al-bearing silicates, because differences in the magnitudes of $f(CO_2)$ and $f(H_2O)$ during low-grade metamorphism (at

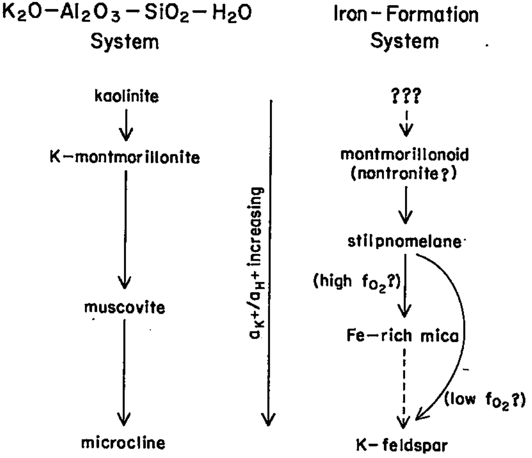

FIG. 10. Schematic diagram showing reaction sequences of Al-bearing silicates in the $K_2O$–$Al_2O_3$–$SiO_2$–$H_2O$ and iron-formations systems. The sequences are arranged downward with increasing $a_{K^+}/a_{H^+}$ at constant T and P. The labels indicating low $f(O_2)$ and high $f(O_2)$ refer to oxygen fugacities nearly defined by the hematite–magnetite and pyrrhotite–pyrite–magnetite assemblages, respectively (see text).

100 to 150°C) are very small (see fugacity data of Ryzhenko & Volkov 1971, Burnham *et al.* 1969, Miyano 1978c). The $f(O_2)$ may also influence the stability ranges of K–Al-bearing silicates. Stilpnomelane–K-feldspar assemblages are not observed in the presence of hematite (+magnetite±pyrite). In contrast, stilpnomelane–Fe-rich mica assemblages do not occur under reducing conditions where pyrrhotite (+pyrite±magnetite) is stable. However, the $f(O_2)$ may not have as influential an effect on the stability sequences as the $a_{K^+}/a_{H^+}$ ratio because, in reactions 2) and 3), an increase or decrease in $f(O_2)$ can be compensated by a decrease or increase in Fe/(Fe+Mg) of stilpnomelane, respectively.

The sequence shown in Figure 10 cannot be observed at one locality. The respective assemblages appear to be a function of the magnitude of $a_{K^+}$, or potassium availability. Differences in $a_{K^+}$ may have had a greater effect on the mineral stabilities than temperature, which may not have differed by more than 10°C across the member. This means that homogenization of $a_{K^+}$, the chemical potential of $K^+$, was incomplete in the iron formation at temperatures of 110 to 150°C (Miyano 1976b, 1978b). Therefore, stable associations of K–Al-bearing minerals are probably maintained through local equilibrium. Considering the intimate association of Fe-rich mica and riebeckite and the replacement of stilpnomelane by riebeckite, as will be discussed below, participation of both potassium and sodium is essential in such associations. However, very few Na-bearing minerals other than riebeckite are found in the BIF. Miyano (1976a) noted authigenic orthoclase in a shale macroband of the Dales Gorge Member. Klein & Fink (1976) reported a small amount of authigenic albite with nearly end-member composition from the Sokoman Iron Formation, which underwent very low grade metamorphism. This suggests that differences in $a_{Na^+}$ similar to those of $a_{K^+}$ may be responsible for the variety of Na-bearing mineral assemblages in rocks of the iron formation.

### *Stilpnomelane–riebeckite association*

The relationship between stilpnomelane and riebeckite is complex. Grubb (1971) reported that riebeckite completely replaces stilpnomelane as a result of interaction with Na-bearing solutions, but he did not evaluate the alumina budget in such a replacement process. Fe-rich mica may be a possible source or sink (or both) for aluminum. Riebeckite generally has a low $Al_2O_3$ content (below 1.0 wt. %: Table 3) and the coexisting stilpnomelane is not enriched in Al. However, Fe-rich mica commonly occurs near or within a riebeckite band or zone. This suggests that, when stilpnomelane is replaced by riebeckite, the Al released has been reprecipitated as Fe-rich mica close to the riebeckite zone. Accordingly, Al may not have traveled farther than about 5 mm from such a band. On account of the deficiency of alkalis in iron formations and the above suggested behavior of Al, additional alkalis for the local crystallization of riebeckite and mica may have been derived from elsewhere in the bulk-rock system, probably through alkali-bearing solutions. Because there are effective impermeable barriers against the migration of aqueous solutions, such as shale macrobands alternating with the BIF, it is possible that differences in $a_{K^+}$ (also $a_{Na^+}$) may have been caused by the difficulty of transport or mobility of alkali-bearing solutions. Much of the crystallization of riebeckite and Fe-rich mica, however, may be related to alkali-bearing solutions derived from deformation as suggested by Trendall & Blockley (1970).

## CONCLUSIONS

Textural relations show that the majority of Al-bearing minerals are of late diagenetic to very low-grade metamorphic origin. The origin of the hornblende is uncertain; it may be authigenic or it may possibly represent volcanic detritus. Its texture and chemical composition are not diagnostic of either mode of origin. The stability relations of Al-bearing minerals are very qualitatively discussed on the basis of possible reactions predicted from mineral assemblages. The formation of stilpnomelane, Fe-rich mica and K-feldspar appears to have been controlled by differences in $a_{K^+}/a_{H^+}$ ratios during very low-grade metamorphism.

The Al-bearing silicates observed in the very weakly metamorphosed iron-formation rocks are not direct indicators of the depositional environments of chemical sediments such as the BIF. However, investigation of the Al-bearing mineral assemblages may provide information on the environmental conditions during late diagenesis or very low-grade metamorphism of the iron-formation rocks.

## ACKNOWLEDGEMENTS

I thank Hancock and Wright Prospecting Pty. Ltd. for permission to collect diamond drill core from the Colonial mine area. Part of this study was supported by Grant-in-Aid for Encouragement of a Young Scientist (574326) of the Ministry of Education, Science and Culture of Japan. Further funding was provided by NSF grant EAR 80-20377 to C. Klein. I used electron microprobes at the Analytical Center of Tsukuba University and at the Geological Survey of Japan. I am much indebted to A. Sasaki and K. Okumura at the Geological Survey of Japan and N. Nishida of Tsukuba University for their help in obtaining microprobe data, to S. Sueno and S. Miyano for obtaining X-ray powder data, to Mrs. Thea Brown for the typing of the manuscript, and to C. Klein for his critical review and constructive suggestions, which considerably improved its content.

## REFERENCES

Ayres, D.E. (1972): Genesis of iron-bearing minerals in banded iron formation mesobands in the Dales Gorge Member, Hamersley Group, Western Australia. *Econ. Geol.* 67, 1214-1233.

Burnham, C.W., Holloway, J.R. & Davis, N.F. (1969): Thermodynamic properties of water to 1,000°C and 10,000 bars. *Geol. Soc. Amer. Spec. Pap.* 132.

Burt, D.M. (1972): The system Fe–Si–C–O–H: a model for metamorphosed iron formations. *Carnegie Inst. Wash. Year Book* 71, 435-443.

Deer, W.A., Howie, R.A. & Zussman, J. (1962): *Rock-Forming Minerals. 3, Sheet Silicates.* Longmans, London.

Dimroth, E. & Chauvel, J.-J. (1973): Petrography of the Sokoman Iron Formation in part of central Labrador Trough, Quebec, Canada. *Geol. Soc. Amer. Bull.* 84, 111-134.

Donnay, G., Morimoto, N., Takeda, H. & Donnay, J.H.D. (1964): Trioctahedral one-layer micas. I. Crystal structure of a synthetic iron mica. *Acta Cryst.* 17, 1369-1373.

Eggleton, R.A. (1972): The crystal structure of stilpnomelane. II. The full cell. *Mineral. Mag.* 38, 693-711.

——— & Chappell, B.W. (1978): The crystal structure of stilpnomelane. III. Chemistry and physical properties. *Mineral. Mag.* 42, 361-368.

Floran, R.J. & Papike, J.J. (1975): Petrology of the low-grade rocks of the Gunflint Iron-Formation. Ontario-Minnesota. *Geol. Soc. Amer. Bull.* 86, 1169-1190.

——— & ——— (1978): Mineralogy and petrology of the Gunflint Iron Formation, Minnesota-Ontario: correlation of compositional and assemblage variations at low to moderate grade. *J. Petrology* 19, 215-288.

Frost, B.R. (1979): Metamorphism of iron-formation: paragenesis in the system Fe–Si–C–O–H. *Econ. Geol.* 74, 775-785.

Gole, M.J. (1980): Mineralogy and petrology of very-low-metamorphic grade Archaean banded iron-formations, Weld Range, Western Australia. *Amer. Mineral.* 65, 8-25.

——— & Klein, C. (1981): Banded iron-formations through much of Precambrian time. *J. Geol.* 89, 169-183.

Grubb, P.L.C. (1971): Silicates and their paragenesis in the Brockman Iron Formation of Wittenoom Gorge, Western Australia. *Econ. Geol.* 66, 281-292.

Helgeson, H.C., Brown, T.H. & Leeper, R.H. (1969): *Handbook of Theoretical Activity Diagrams Depicting Chemical Equilibria in Geologic Systems Involving an Aqueous Phase at One Atm and 0° to 300°C.* Freeman, Cooper & Company, San Francisco.

Hemley, J.J. (1959): Some mineralogical equilibria in the system $K_2O$–$Al_2O_3$–$SiO_2$–$H_2O$. *Amer. J. Sci.* 257, 241-270.

James, H.L. & Sims, P.K. (1973): Precambrian iron-formations of the world, Introduction. *Econ. Geol.* 68, 913-914.

Klein, C., Jr. (1974): Greenalite, stilpnomelane, minnesotaite, crocidolite and carbonates in a very low-grade metamorphic Precambrian iron-formation. *Can. Mineral.* 12, 475-498.

——— & Fink, R.P. (1976): Petrology of the Sokoman Iron Formation in the Howells River area, at the western edge of the Labrador trough. *Econ. Geol.* 71, 453-487.

——— & Gole, M.J. (1981): Mineralogy and petrology of parts of the Marra Mamba Iron-Formation, Hamersley Basin, Western Australia. *Amer. Mineral.* 66, 507-525.

LaBerge, G.L. (1966): Altered pyroclastic rocks in iron-formation in the Hamersley Range, Western Australia. *Econ. Geol.* 61, 147-161.

Lesher, C.M. (1978): Mineralogy and petrology of the Sokoman Iron Formations near Ardua Lake, Quebec. *Can. J. Earth Sci.* 15, 480-500.

Milton, C. & Eugster, H.P. (1959): Mineral assemblages of the Green River Formation. *In* Researches in Geochemistry (P.H. Abelson, ed.). John Wiley & Sons, New York.

Miyano, T. (1976a): Mineral assemblages of the Proterozoic banded iron formation in the Hamersley area. *Mining Geol. Japan* 26, 273-288.

——— (1976b): Physicochemical environments during burial metamorphism of the Dales Gorge Member, Hamersley Group, Western Australia. *Mining Geol. Japan* **26**, 311-325.

——— (1978a): Effect of $CO_2$ on mineralogical differences in some low-grade metamorphic iron formations. *Geochem. J. Japan* **12**, 201-211.

——— (1978b): Phase relations in the system Fe–Mg–Si–O–H and environments during low-grade metamorphism of some Precambrian iron formations. *J. Geol. Soc. Japan* **84**, 679-690.

——— (1978c): Stability relations of iron-bearing minerals in the $H_2O$–$CO_2$ mixed-volatile region at lower temperatures. *J. Geol. Soc. Japan* **84**, 711-719.

MUELLER, R.F. (1960): Compositional characteristics and equilibrium relations in mineral assemblages of a metamorphosed iron formation. *Amer. J. Sci.* **258**, 449-497.

RYZHENKO, B.N. & VOLKOV, V.P. (1971): Fugacity coefficients of some gases in a broad range of temperatures and pressures. *Geochem. Int.* **8**, 468-481.

SUDO, T. (1974): *Clay Mineralogy*. Iwanami Book Co., Tokyo.

TRENDALL, A.F. & BLOCKLEY, J.G. (1970): The iron formations of the Precambrian Hamersley Group, Western Australia, with special reference to the associated crocidolite. *West. Aust. Geol. Surv. Bull.* **119**.

WONES, D.R. (1963): Phase equilibria of 'ferri-annite' $KFe^{+2}_3Fe^{+3}Si_3O_{10}(OH)_2$. *Amer. J. Sci.* **261**, 581-596.

*Received August 1981, revised manuscript accepted February 1982.*